25 November 1994

ELSEVIER

Chemical Physics Letters 230 (1994) 276–282

CHEMICAL PHYSICS LETTERS

Angle-differential electron energy spectra for the autoionization systems He*(2 ^{1}S)+H/D(1 ^{2}S). Comparison between ab initio theory and experiment

M. Movre [a,1], W. Meyer [a], A. Merz [b], M.-W. Ruf [b], H. Hotop [b]

[a] *Fachbereich Chemie, Universität Kaiserslautern, D-67653 Kaiserslautern, Germany*

[b] *Fachbereich Physik, Universität Kaiserslautern, D-67653 Kaiserslautern, Germany*

Received 19 July 1994; in final form 22 September 1994

Abstract

We present angle-dependent electron energy spectra due to ionizing collisions of metastable He*(2 ^{1}S) atoms with ground-state hydrogen and deuterium atoms. The data, measured at thermal collision energies ($E_{rel} \approx 50$ meV), show an angular variation of the spectral shape which is well reproduced by a quantum-mechanical calculation based on local complex potential theory. The ab initio calculated resonance-to-continuum complex coupling elements show a strong dependence on the electronic structure of the quasi-molecule and its changes with internuclear separation. Therefore the total autoionization width shows a significant deviation from a damped exponential shape. Autoionization occurs dominantly into the (molecule fixed) electronic p wave. Calculated total autoionization cross sections are 84 Å^2 at $E_{rel} = 50$ meV, and follow approximately a $E_{rel}^{-0.5}$ decay for larger energies. At $E_{rel} = 50$ meV, associative and quasi-associative processes account for about 12% and 4%, respectively, of the total cross section.

1. Introduction

The dynamics of autoionizing collision complexes involving metastable helium atoms has been the subject of many studies, as reviewed in Refs. [1–3]. In particular, detailed information has been obtained for the fundamental prototype systems He*(2 ^{3}S)+H/D(1 ^{2}S) [4–10]. Collisions between helium atoms in the energetically higher-lying 2 ^{1}S state and atomic hydrogen have also been the subject of quite a few investigations [11–22], but they have not – at least not electron-spectroscopically – been studied in the same detail as the triplet system.

So far, the electron spectrum for the system He*(2 ^{1}S)+H(1 ^{2}S) has been recorded at a single fixed detection angle (perpendicular to the crossed atomic beams) [11,14]. Reflecting the relevant variation in the difference potential $V^*(R) - V^+(R)$ of entrance and exit channels, the spectrum extends over an energy range of about 0.6 eV, much less than the 4 eV range of the He*(2 ^{3}S)+H(1 ^{2}S) spectrum [4–8,10,11,14]. In contrast to the latter case, the published electron spectra for He*(2 ^{1}S)+H(1 ^{2}S) display little structure and are characterized by a single Airy-type peak as associated with a local minimum in the difference potential (see Fig. 1 below). From the low energy edge of the experimental spectrum, a well depth $D_e^* = 0.46(5)$ eV has been deduced [11] for the He*(2 ^{1}S)+H(1 ^{2}S) $^2\Sigma^+$ entrance channel

[1] Permanent address: Institute of Physics, University of Zagreb, 41000 Zagreb, Croatia.

0009-2614/94/$07.00 © 1994 Elsevier Science B.V. All rights reserved
SSDI 0009-2614(94)01157-5

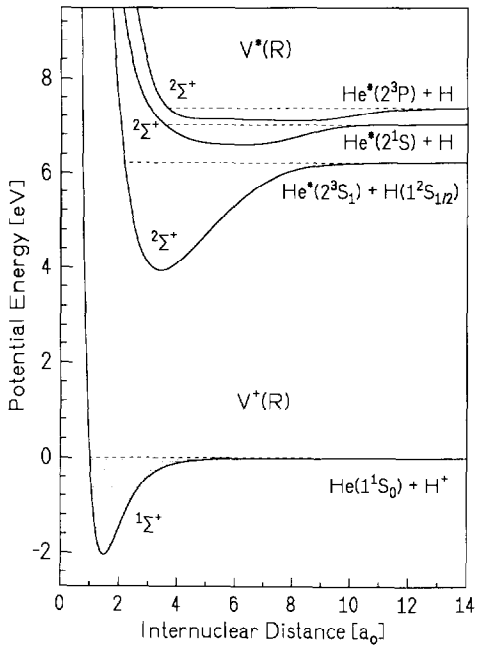

Fig. 1. Potential curves relevant for the autoionization processes He*($2\,^1$S, $2\,^3$S)+H/D($1\,^2$S)→He+H$^+$/D$^+$+e$^-$ (taken from Ref. [10]).

potential, somewhat larger than previous ab initio values of $D_e^* = 0.39$ eV and 0.35 eV (Refs. [18,21], respectively, see also Ref. [16]).

Khan et al. [15,16] measured the angle-dependent energy spectra of H$^+$/D$^+$ ions resulting from He*($2\,^1$S)+H/D collisions at an average kinetic energy of 400 meV. For comparison they carried out quantum mechanical calculations [16] based on ab initio results for the potentials $V^*(R)$ [18,21], $V^+(R)$ [23] and the autoionization width $\Gamma(R)$ [21]. They found that the theoretical ion angular distribution was more strongly forward-peaked than the experimental result (this difference was later linked to angular momentum exchange between the electron and the heavy particle system [3]) and that the calculated ion recoil energy distribution peaked at higher energy (shifted by about 0.11 eV) than the experimental spectrum. Khan et al. [16] attributed the latter discrepancy to processes involving nonadiabatic coupling of the $^2\Sigma^+$ entrance channel correlating to the He*($2\,^1$S)+H asymptote with the channel arising from He*($2\,^3$P)+H. In order to arrive at a satisfactory description of both the ion and electron spectra, they substantially modified the ab initio potentials for the two entrance channels in particular in the region of their avoided crossing. They arrived at a well depth of $D_e^* = 0.44(4)$ eV as had been suggested from the earlier experimental result [11].

In this Letter, we continue our work on the autoionization dynamics of simple Penning ionization (PI) systems with emphasis on angular-dependent electron spectra [5–8,10,24]. First we discuss the theoretical treatment which includes ab initio calculated complex entrance channel potentials and electron angular momentum dependent autoionization amplitudes. After a brief description of relevant experimental details, we report the angle-dependent experimental and theoretical electron energy spectra for He*($2\,^1$S)+H and D. The angular variations of the respective spectral shapes are discussed.

2. Theoretical treatment

The methods used are those presented in detail in Ref. [10] and may be summarized as follows. The autoionizing resonance states are defined through Feshbach projection based on orbital occupancy, and the corresponding potentials are determined by use of MR-CI with an accuracy of about 10 meV. These CI calculations started from MC-SCF wavefunctions optimized in the space of fourteen $^2\Sigma^+$ configurations (for details see Ref. [10]), providing an adequate description of the four states correlating to the asymptotes with He in the states $2\,^3$S, $2\,^1$S and $2\,^3$P, $2\,^1$P, respectively. The orbitals have been determined to make the energy average of the two lower resonance states stationary. Fig. 1 reproduces the potential curves which are relevant for the processes He*($2\,^1$S, $2\,^3$S)+H/D($1\,^2$S)→He+H$^+$/D$^+$+e$^-$ as given in Ref. [10]. The potentials exhibit a series of avoided crossings caused by the ionic structure corresponding to He$^+$+H$^-$. The $^2\Sigma^+$ entrance channel potential stemming from the He*($2\,^1$S)+H/D($1\,^2$S) asymptote has a broad and shallow well with an equilibrium internuclear distance of $R_e = 6.0\ a_0$ and a depth of $D_e = 0.426 \pm 0.010$ eV. The latter value is consistent with the experimental estimates [11,16]. The pseudocrossing with the higher He*($2\,^3$P)+H/D($1\,^2$S) $^2\Sigma^+$ potential at around $R = 9\ a_0$ causes the peculiar shape of the latter. We observe that our re-

sults do not support the drastic ad hoc modifications of the two potentials in Ref. [6] which resulted in a sharply avoided crossing with a minimal energy separation of about 35 meV. In fact, the two states show a rather flat crossing and always stay apart by more than 200 meV. For collision energies which are relevant to our experiment, only a small fraction of collision complexes will access the upper state. Therefore we shall not consider nonadiabatic couplings between these two states. Analysis of the electronic wavefunctions and corresponding dipole moments reveals that there is a further avoided crossing of these two states at around $R \approx 3.5\ a_0$.

The energy-dependent coupling with the autoionization continuum is determined as part of the Feshbach projected MR-CI and is cast in the form of a compact (L^2) 'Penning MO' without any phase information being lost [10]. This MO is then projected onto the states of the continuum electron in the exit channel with energy $\epsilon(R) = V^* - V^+(R)$. The continuum states are determined numerically within the static-exchange approximation by a single-center partial wave expansion which produces a set of coupled equations for radial components. We have used up to 17 coupled angular momentum channels in order to obtain well converged results for the complex coupling matrix elements $V_l(R)$ for distances up to $R \approx 10\ a_0$. Fig. 2a displays our ab initio V_l referring to the center-of-mass of the He*($2\,^1$S)+H($1\,^2$S) and He*($2\,^1$S)+D($1\,^2$S) collisional complexes. The slight differences between the two isotopic systems are entirely due to the different locations of the corresponding centers of mass. The coupling matrix elements exhibit a drastic change at around $R = 3.5\ a_0$ due to their strong dependence on the electronic structure of the resonance state. The resulting partial autoionization widths $\Gamma_l(R) = 2\pi |V_l(R)|^2$ for He*($2\,^1$S)+H and D are shown in Fig. 2b. In both cases the electronic p wave provides the dominant contribution to the total autoionization width. The total width shows a significant deviation from a simple exponential shape. For comparison, we include the total width calculated by Isaacson and Miller [21] in Fig. 2b. The two curves are close to each other for internuclear distances $R \geq 4\ a_0$ which are probed in our experiment, but the present width exhibits a local minimum at $R \approx 3.25\ a_0$ and increases again for shorter distances while the width function of Isaacson and Miller shows a maximum at $R = 3\ a_0$.

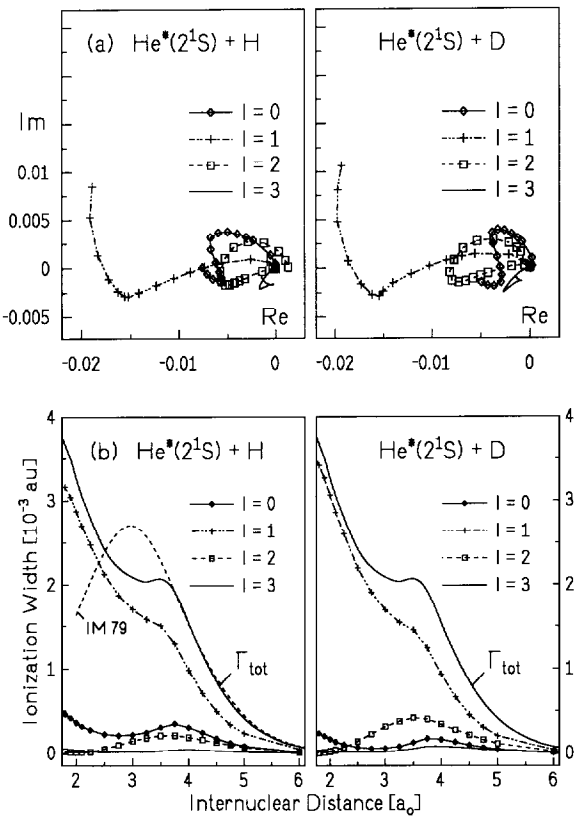

Fig. 2. (a) Ab initio complex coupling matrix elements $V_l(R)$, calculated for the internuclear separations $R = 2$ to $5.0\ a_0$ in steps of $\Delta R = 0.25\ a_0$ and from $R = 5.0$ to $9.0\ a_0$ in steps of $\Delta R = 1\ a_0$. (b) Partial autoionization widths $\Gamma_l(R)$. The total autoionization width Γ_{tot} of Ref. [21] is included for comparison (IM 79, dashed line) with the present result (solid line).

The heavy particle motion in the local potentials $V^* - \frac{1}{2}i\Gamma$ and V^+ is treated by a complex Numerov algorithm as discussed in detail in Ref. [10]. Autoionization cross sections are then calculated using a converged set of complex coupling matrix elements $V_l(R)$. By proper weighting with the experimental collision energy distribution and convolution with the experimental electron energy resolution we finally obtain theoretical angle-dependent spectra for Penning and associative ionization processes in He*($2\,^1$S)+H/D($1\,^2$S) which can be directly compared to experiment. They are displayed in Figs. 4 and 5 and will be discussed in Section 4 together with

our results for total and partial ion production cross sections.

3. Experiment

Our apparatus, as described in detail in Refs. [6,8], involves crossed atomic beams and two double-hemispherical condensers for electron detection. One of the spectrometers detects charged particles at $\Theta = 90°$ with respect to both atomic beams and serves as a monitor detector. Its detection geometry corresponds to the one used in all previous work [4,14,25]. The second spectrometer is rotatable and detects electrons in the collision plane spanned by the atomic beams. Both detectors are operated at a fixed transmission energy of 4.8 eV leading to an effective resolution of about 30 meV.

The metastable helium atoms are produced in a differentially pumped cold cathode dc discharge. The resulting beam contains helium atoms in the $2\,^3S$ and in the $2\,^1S$ state, favouring the triplet species by 8:1 [6]. The $2\,^1S$ flux is estimated to be $2 \times 10^{14}\,s^{-1}\,sr^{-1}$. The average metastable velocity is $\bar{v}_{He} = 1750$ m/s and the distribution has a width of $\Delta v/\bar{v}_{He} \approx 30\%$ [8]. The atomic hydrogen beam is produced in an air-cooled microwave discharge outside the vacuum chamber and guided to the reaction zone by a PTFE-covered stainless steel tube, yielding an effective density ratio of $n(H)/n(H_2) \approx 0.2$. Its velocity distribution can be assumed to be a Maxwellian for an effusive quasi beam ($T = 300$ K, $\bar{v}_H = 2500$ m/s, $\bar{v}_D = 1770$ m/s) [6,8].

Electron spectra due only to $He^*(2\,^1S)$-induced ionization processes (as shown in Fig. 3) are produced as follows: we selectively and nearly completely ($\geq 99.5\%$) remove $2\,^1S$ atoms from the mixed $He^*(2\,^1S, 2\,^3S)$ beam by irradiation of light from a He discharge lamp surrounding the metastable He^* beam [6,8,11] and subtract the resulting pure $2\,^3S$ spectra from mixed $(2\,^1S, 2\,^3S)$ spectra, as accumulated for an equal time interval and equivalent conditions. The statistical uncertainty of the ^1S results is somewhat larger than for the corresponding ^3S spectra [6–8], but the background regions for energies lower than 6.4 eV and higher than 7.3 eV provide a reliable measure of the size of possible artificial features (see Fig. 3).

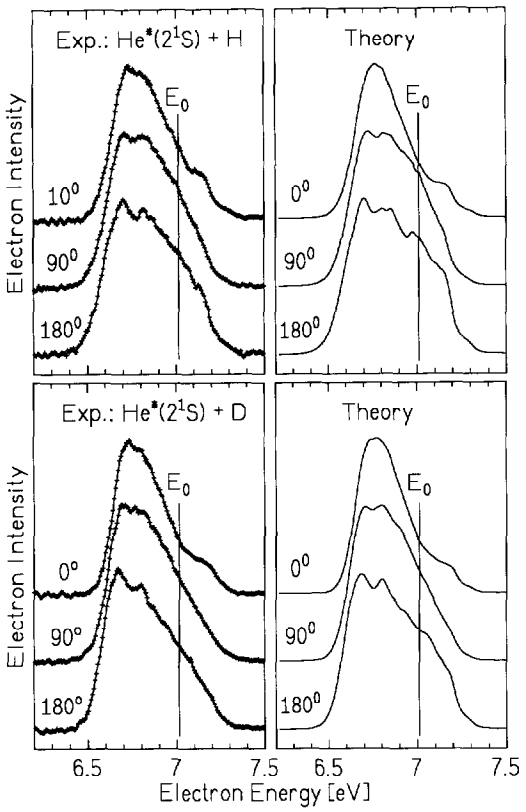

Fig. 3. Experimental (left) and theoretical (right) electron energy spectra for the autoionization complexes $He^*(2\,^1S)+H$ (upper) and $He^*(2\,^1S)+D$ (lower). The corresponding detection angles $\Theta = 10°$ (0°), 90° and 180° refer to the average relative velocity vectors v_{rel} ($He^* \rightarrow H/D$) of the respective velocity distributions of the atomic beams. The energies E_0 correspond to the differences between the $He^*(2\,^1S)$ excitation energy and the ionization energy of $H(1\,^2S)$ (7.018 eV) or $D(1\,^2S)$ (7.015 eV), respectively.

4. Results and discussion

Fig. 3 shows three experimental (left panels) and theoretical (right panels) electron energy spectra for the autoionization processes $He^*(2\,^1S)+H$ (upper panels) and D (lower panels) for the detection angles $\Theta = 10°$ (0°), 90° and 180°. Closer inspection reveals that the singlet spectra vary with the detection angle, although to a smaller extent than we have observed for the triplet spectra [6–8,10]. The experimental H, as well as the D spectrum for forward electron emission ($\Theta = 10°/0°$) shows a shoulder close to the energies $E_0 + \bar{E}_{rel} = 7.018\ (7.015) + 0.05$

eV which separate approximately the contributions due to Penning ($E_{el} \leqslant E_0 + \bar{E}_{rel}$) and associative ($E_{el} \geqslant E_0 + \bar{E}_{rel}$) ionization. The overall form of the distributions as well as the shoulder are well reproduced by the quantum mechanical ab initio calculations. The width of the experimental spectra (taken as the full width at half maximum) increases from 380 (330) meV at $\Theta = 10°$ (0°) to 530 (480) meV at $\Theta = 180°$ for H(D), in full agreement with the calculations. For larger detection angles an additional structure appears in the maximum of the spectra. The nice agreement with the theoretical spectra proves that the local minimum in the center of the experimental peak – particulary clearly seen for both isotopes in backward detection direction – is a real structure. In fact, from the calculations it can be easily extracted that this structure is the signature of the 'fast' oscillations in the entrance channel which are due to the interference of incoming and outgoing waves [5,10].

The internal angular distributions (IAD) for electron emission from the quasi-molecule [He*(2 ^{1}S)H/D]*, i.e. the angle dependent electron intensity as emitted in the frame of the autoionizing collisional complex for fixed internuclear separation R, is given in terms of the coupling elements V_l by

$$I_{IAD}(\vartheta) \propto \left| \sum_l i^{-l} Y_{l0}(\vartheta) V_l(R) \right|^2 ,$$

where ϑ represents the body-fixed electron emission angle. Fig. 4 shows the results of the ab initio calculation of the IAD for small ($R = 3.0\ a_0$, $3.25\ a_0$ and $R = 3.5\ a_0$) and intermediate ($3.75\ a_0 \leqslant R \leqslant 5\ a_0$, $\Delta R = 0.25\ a_0$) internuclear distances. For short distances the distribution varies strongly with R: at $R = 3\ a_0$ the forward intensity is larger than the backward peak, but with growing internuclear distance the forward maximum is strongly reduced so that for $R \geqslant 3.5\ a_0$, i.e. the experimentally relevant internuclear distances, the backward maximum dominates the shape of the IAD. This is compatible with the observed angle-dependent changes of the experimental spectra in the AI region. At this point we should note that even in this case of a strongly anisotropic IAD distribution, the electron spectrum taken perpendicular ($\Theta = 90°$) to both beams is in close agreement with a theoretical angle-integrated spectrum derived under

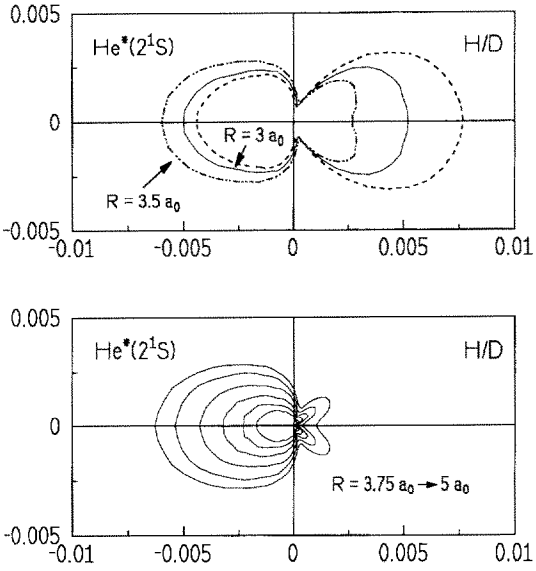

Fig. 4. Internal angular distribution of electron emission by the collision complexes [He*(2 ^{1}S) – H/D]* from ab initio calculations for short internuclear separations $R = 3.0$, 3.25 and 3.5 a_0 (upper part) and for intermediate separations $R = 3.75$ to 5.0 a_0 in steps of $\Delta R = 0.25\ a_0$ (lower part). The intensity scale is proportional to the autoionization width $\Gamma(R)/2\pi$ (au).

the simplifying assumption of $\Delta J = 0$ and emission of s-wave electrons only, that is $V_l = \delta_{l0}(\Gamma/2\pi)^{-1/2}$, as has been found for other attractive Penning ionization systems [5,24].

Finally we present the dependence of total (σ_{TI}) and partial (σ_{PI}, σ_{AI}, σ_{QI}) ion production cross sections for He*(2 ^{1}S) + H on the collision energy E_{rel} in the range 7–130 meV (see Fig. 5). For a discussion of previous work we refer the reader to Refs. [10,16,22]; in connection with the characteristics of total and partial ion production, including the formation of quasi-bound HeH^+ states (σ_{QI}), we note the detailed discussion for the system He*(2 ^{3}S) + H given in Ref. [4].

The total ionization cross section σ_{TI} decreases weakly, but monotonically with rising E_{rel} and decays as $E_{rel}^{-0.5}$ at the highest energies. It amounts to 84 Å^2 at $E_{rel} = 50$ meV, i.e. our experimental mean collision energy. The absolute cross section $\sigma_{TI} = 71$ Å^2 ($\pm 20\%$), determined by Morgner and Niehaus [14] an average collision energy of $\bar{E}_{rel} = 45$ meV, is compatible with our theoretical result. The cross section for Penning ionization (i.e. for proton production)

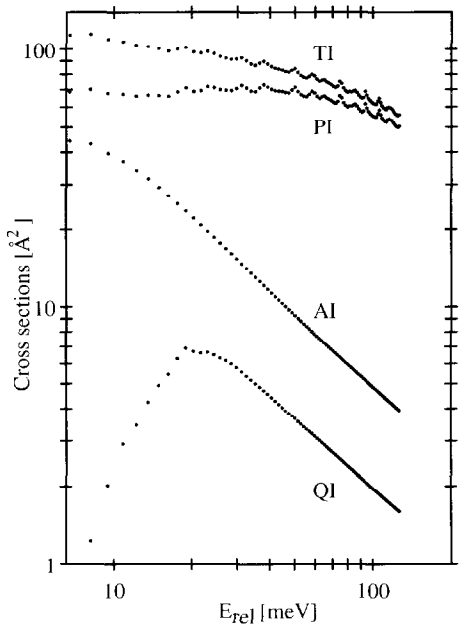

Fig. 5. Theoretical results for the total and partial ionization cross sections in $He^*(2\,^1S)+H(1\,^2S)$ collisions for energies between 7 and 130 meV. σ_{TI}: total ionization; σ_{PI}: Penning ionization (formation of H^+); σ_{AI}: associative ionization (formation of stable HeH^+ ions); σ_{QI}: ionization into quasi bound HeH^+ ions (lifetimes not specified, see Ref. [4] for more details).

is nearly constant in the range 8–50 meV and then decreases in a fashion similar to σ_{TI}. The PI cross sections show pronounced sawtooth structures (width $\approx$ 10 meV) which, to our knowledge, have not yet been observed in PI experiments. As discussed in detail for the $He(2\,^3S)$ case [10], they are related to the oscillations of barrier transmission in the vicinity of the peak of the centrifugal barrier. The cross section for associative ionization (σ_{AI}), i.e. for the formation of stable $HeH^+(v^+, J^+)$ ions, accounts for as much as 38% of σ_{TI} at $E_{rel}=8$ meV ($\sigma_{AI}=43$ Å^2) but decreases strongly with rising collision energies (approximately as $E_{rel}^{-0.94}$). At $E_{rel}=50$ meV the ratio σ_{AI}/σ_{TI} amounts to 12%, in agreement with the ion data of Fort et al. [13]. Averaging with our collision energy distribution leads to a fraction of 15% for associative ionization. For comparison, we estimate the fraction of AI processes from our high-resolution spectrum ($\Theta=90°$) by imposing the criterion $\epsilon \geqslant E_0 + \langle E_{rel} \rangle$. Due to the fact that σ_{AI} and σ_{TI} show different dependences on E_{rel}, an estimate based on the choice $\langle E_{rel} \rangle = \bar{E}_{rel} = 50$ meV results in too low a value (AI fraction 11%$\pm$2%); with the more appropriate choice $\langle E_{rel} \rangle = 30$ meV we estimate an AI fraction of 13%$\pm$2%. This value is compatible with the theoretical average for our collision energy distribution. As to be expected from the close agreement in total ionization widths for $R \geqslant 4\ a_0$, our results for σ_{TI} and σ_{AI} agree well with those of Isaacson [22].

The cross section σ_{QI} for the formation of quasi-bound HeH^+ states with energies in the $He-H^+$ continuum, but trapped in the rotational barrier of the effective ionic potential, rises strongly at low energies, reaches a maximum near $E_{rel}=20$ meV ($\sigma_{QI}=7$ Å^2) and then decreases in a similar way as σ_{AI}. At 50 meV, σ_{QI} amounts to 4.2% of σ_{TI}. Under our beam conditions, QI then accounts for $\approx$ 5% of the ion production but note that due to the short lifetime of the majority of the resonances (see Ref. [4]) these processes will mainly be observed as part of the Penning ion production.

Our cross sections were obtained within the two-state approximation, i.e. we considered autoionization from the $He^*(2\,^1S)+H(^2\Sigma^+)$ entrance channel to the final $HeH^+(^1\Sigma^+)$ channel and ignored couplings to the $^2\Sigma^+$ channel arising from $He^*(2\,^3P)+H$ (see Fig. 1). As argued above, this approximation is justified for our experimental collision energies.

We note that Khan et al. [16] have obtained total and partial ion production cross sections, as based on their modified $^2\Sigma^+$ entrance channel potential and including nonadiabatic couplings, which are substantially lower than our and Isaacson's [22] results. As mentioned in Section 2, their modifications of the potentials are not supported by the present accurate ab initio calculations. We intend to investigate the role of nonadiabatic couplings in future calculations dealing with collisions at energies above 200 meV.

5. Concluding remarks

We have presented experimental and theoretical work on the Penning and associative ionization processes $He^*(2\,^1S)+H/D(1\,^2S)$. Quantum mechanical calculations based on accurate ab initio potentials and complex resonance-to-continuum coupling elements are in agreement with angle-differential, high-resolution experimental electron spectra. The ab initio calculation reveals a strong dominance of au-

toionization into the electronic p wave. We conclude that local complex potential theory in the frame of the Born–Oppenheimer approximation provides a valid approach for the description of the autoionization process in $He^*(2\,^1S)+H/D(1\,^2S)$ collisions, provided that phase relations of the coupling elements are retained and the electron angular momentum transfer is fully included.

Acknowledgement

This work has been supported by the Deutsche Forschungsgemeinschaft (SFB 91 and Ho 427/19-1) and through Graduiertenkolleg 'Laser- und Teilchenspektroskopie'. One of us (MM) acknowledges the hospitality of Fachbereich Chemie and Fachbereich Physik at the University of Kaiserslautern and financial support by the Deutsche Forschungsgemeinschaft (436 KRO-17).

References

[1] A. Niehaus, Phys. Rept. 186 (1990) 149.
[2] E.G. Brunetti and F. Vecchiocattivi, in: Current topics in ion chemistry and physics (Wiley, New York, 1993).
[3] P.E. Siska, Rev. Mod. Phys. 65 (1993) 337.
[4] H. Waibel, M.-W. Ruf and H. Hotop, Z. Physik 9 (1988) 191.
[5] A. Merz, M.W. Müller, M.-W. Ruf, H. Hotop, W. Meyer and M. Movre, Chem. Phys. 145 (1990) 219.
[6] A. Merz, M.-W. Ruf and H. Hotop, Phys. Rev. Letters 69 (1992) 3467.
[7] A. Merz, M.-W. Ruf, H. Hotop, M. Movre and W. Meyer, in: AIP Conference Proceedings 295, The physics of electronic and atomic collisions, Proc. XVIIIth ICPEAC, Aarhus, Denmark, 1993, eds. T. Andersen, B. Fastrup, F. Folkmann, H. Knudsen and N. Andersen (AIP Press, New York, 1993) p. 852.
[8] A. Merz, M.-W. Ruf, H. Hotop, M. Movre and W. Meyer, submitted for publication.
[9] B. Sarpal, J. Phys. B 26 (1993) 4145.
[10] M. Movre and W. Meyer, submitted for publication.
[11] H. Hotop, E. Illenberger, H. Morgner and A. Niehaus, Chem. Phys. Letters 8 (1971) 493.
[12] J.S. Howard, J.P. Riola, R.D. Rundel and R.F. Stebbings, J. Phys. B 6 (1973) L109.
[13] J. Fort, J.J. Laucagne, A. Pesnelle and G. Watel, Phys. Rev. A 14 (1976) 658.
[14] H. Morgner and A. Niehaus, J. Phys. B 12 (1979) 1805.
[15] A. Khan, S. Siddiqui, D.W. Martin and P.E. Siska, Chem. Phys. Letters 84 (1981) 280.
[16] A. Khan, H.R. Siddiqui and P.E. Siska, J. Chem. Phys. 94 (1991) 2588.
[17] H. Fujii, H. Nakamura and M. Mori, J. Phys. Soc. Japan 29 (1970) 1030.
[18] W.H. Miller and H.F. Schaefer III, J. Chem. Phys. 53 (1970) 1421.
[19] J.S. Cohen and N.F. Lane, J. Phys. B 6 (1973) L113.
[20] A.P. Hickman and H. Morgner, J. Chem. Phys. 67 (1977) 5484.
[21] A.D. Isaacson and W.H. Miller, Chem. Phys. Letters 62 (1979) 374.
[22] A.D. Isaacson, J. Chem. Phys. 71 (1979) 180.
[23] W. Kolos and J.M. Peek, Chem. Phys. 12 (1976) 381.
[24] A. Merz, M.W. Müller, M.-W. Ruf, H. Hotop, W. Meyer and M. Movre, Chem. Phys. Letters 160 (1989) 377.
[25] J. Lorenzen, H. Morgner, W. Bußert, M.-W. Ruf and H. Hotop, Z. Physik A 310 (1983) 141.